



Published in final edited form as:

Cell. 2014 December 4; 159(6): 1312–1326. doi:10.1016/j.cell.2014.11.018.

Tissue-Resident Macrophage Enhancer Landscapes Are Shaped by the Local Microenvironment

Yonit Lavin^{1,3}, Deborah Winter^{2,3}, Ronnie Blecher-Gonen^{2,3}, Eyal David², Hadas Keren-Shaul², Miriam Merad^{1,4,*}, Steffen Jung^{2,4,*}, and Ido Amit^{2,4,*}

¹Department of Oncological Sciences, Immunology Institute and the Tisch Cancer Institute, Icahn School of Medicine at Mount Sinai, New York, NY 10029, USA

²Department of Immunology, Weizmann Institute of Science, Rehovot 76100, Israel

SUMMARY

Macrophages are critical for innate immune defense and also control organ homeostasis in a tissue-specific manner. They provide a fitting model to study the impact of ontogeny and microenvironment on chromatin state and whether chromatin modifications contribute to macrophage identity. Here, we profile the dynamics of four histone modifications across seven tissue-resident macrophage populations. We identify 12,743 macrophage-specific enhancers and establish that tissue-resident macrophages have distinct enhancer landscapes beyond what can be explained by developmental origin. Combining our enhancer catalog with gene expression profiles and open chromatin regions, we show that a combination of tissue- and lineage-specific transcription factors form the regulatory networks controlling chromatin specification in tissue-resident macrophages. The environment is capable of shaping the chromatin landscape of transplanted bone marrow precursors, and even differentiated macrophages can be reprogrammed when transferred into a new microenvironment. These results provide a comprehensive view of macrophage regulatory landscape and highlight the importance of the micro-environment, along with pioneer factors in orchestrating identity and plasticity.

INTRODUCTION

Macrophages are hematopoietic cells of the myeloid lineage that are specialized in phagocytosis and respond to diverse environmental signals (Epelman et al., 2014; Ginhoux and Jung, 2014; Lavin and Merad, 2013; van Furth et al., 1972). They actively maintain steady state by secreting and responding to cytokines and chemokines (Mortha et al., 2014;

©2014 Elsevier Inc.

*Correspondence: miriam.merad@mssm.edu (M.M.), s.jung@weizmann.ac.il (S.J.), ido.amit@weizmann.ac.il (I.A.).

³Co-first author

⁴Co-senior author

ACCESSION NUMBERS

The main GEO accession number for the raw and processed sequencing data reported in this paper is GSE63341, with the subseries accession numbers GSE63338, GSE63339, and GSE63340 for ATAC-seq, ChIP-seq, and RNA-seq, respectively.

SUPPLEMENTAL INFORMATION

Supplemental Information includes Extended Experimental Procedures, seven figures, one data file, and seven tables and can be found with this article online at <http://dx.doi.org/10.1016/j.cell.2014.11.018>.

Zigmond et al., 2014). In addition, tissue-resident macrophages play important homeostatic roles, depending on the tissue in which they reside. Microglia, the brain-resident macrophages, prune synapses during development (Paolicelli et al., 2011; Schafer et al., 2012). Spleen red pulp macrophages phagocytose erythrocytes and recycle heme to maintain iron homeostasis (Chow et al., 2013; Kohyama et al., 2009). Peritoneal cavity macrophages regulate the production of gut immunoglobulin (Ig) A by interacting with peritoneal B1 cells (Okabe and Medzhitov, 2014). These studies, among others, highlight the plasticity of macrophages and their specialization to fulfill tissue-specific functions.

Recent studies have demonstrated that most tissues are populated early during fetal development by macrophages that subsequently maintain themselves, independently of adult hematopoiesis, through longevity and limited self-renewal (Ginhoux et al., 2010; Hashimoto et al., 2013; Schulz et al., 2012; Yona et al., 2013). Thus, most macrophages, although sharing a common lineage, take residence in tissues early during embryogenesis, and the respective macrophage compartments develop locally and independently from each other. A notable exception from this scheme is macrophages residing in the intestine, as these cells are constantly replenished from monocytes even in steady state (Bain et al., 2014; Bogunovic et al., 2009; Varol et al., 2009). Thus, distinct ontogeny is one defining feature of macrophages, but it is unclear to what extent it shapes macrophage identity.

Emerging evidence indicates that environmental factors influence the specialization of tissue-resident macrophages. Heme has been shown to induce Spi-c, a transcription factor (TF) important for red pulp macrophage development (Haldar et al., 2014; Kohyama et al., 2009). Retinoic acid (RA) stimulates Gata6 expression and thereby contributes to the regulatory program of peritoneal macrophages (Okabe and Medzhitov, 2014). Finally, TGF- β was shown to regulate a microglia expression program through Smad TFs (Abutbul et al., 2012; Butovsky et al., 2014). These limited reports provide evidence that environment can govern the expression of tissue-specific macrophage signatures.

Epigenetic modification is one conduit through which ontogeny and environment can influence the development of macrophage identities. The chromatin landscape, among other epigenomic features of a differentiated cell type, reflects both its developmental origin, as well as its future potential (Lara-Astiaso et al., 2014; Stergachis et al., 2013; Winter and Amit, 2014). Nucleosomes are the fundamental unit of chromatin consisting, of ~ 147 bases of DNA wrapped around a histone core. Nucleosome-depleted regions, known as “open chromatin,” contain regulatory elements — such as promoters and enhancers — that play a critical role in gene regulation (Gross and Garrard, 1988). Changes enacted by chromatin remodelers, such as nucleosome eviction or insertion, as well as the addition or deletion of histone modifications, have been linked to changes in the expression of nearby genes (Cirillo et al., 2002; Felsenfeld and Groudine, 2003). Many regulatory modifications are ubiquitous, but variations on a global scale generate the distinct chromatin landscape observed between cell types (Ernst et al., 2011; Heintzman et al., 2009).

During development, pioneer TFs initiate chromatin accessibility to allow the binding of additional TFs (Cirillo et al., 2002; Garber et al., 2012). PU.1 has been implicated as a pioneering factor throughout hematopoietic development, especially in the myeloid lineage.

In macrophages, PU.1 occupies most enhancers, where it is necessary for the maintenance of methylation on the fourth lysine of the H3 subunit (H3K4me1) (Ghisletti et al., 2010; Heinz et al., 2010). The cobinding of PU.1 with line-age-specific TFs orchestrates cell-type specificity by regulating expression and establishing the chromatin landscape (Heinz et al., 2010; Laslo et al., 2006). Cell-type-specific responses to stimuli are largely coordinated through activation by stimulus-triggered TFs that frequently bind to previously occupied “poised” enhancers (Garber et al., 2012; Ostuni et al., 2013). Poised enhancers may reflect past activity and persist throughout development or arise during lineage specification (Lara-Astiaso et al., 2014). Active enhancers mark the current state of a cell and can be distinguished by the presence of acetyl groups on the histone tails, particularly H3K27ac (Creyghton et al., 2010; Heintzman et al., 2007). Tissue-resident macrophages provide a fitting model for examining how chromatin is programmed through development to allow for plasticity within a cell type to specify tissue-specific functions.

Here, we profile the expression and chromatin landscape of seven populations of mouse macrophages isolated from distinct tissues to determine the contributions of ontogeny and environment to tissue-resident macrophage identity. Based on the distribution of histone modifications, we map the regulatory elements of tissue-resident macrophages, including promoters, active enhancers, and poised enhancers. We compare candidate enhancers marked with H3K4me1 in different macrophage populations with those found in monocytes or neutrophils. Through analyzing the distinct enhancer landscape of tissue-resident macrophages, we assess the impact of developmental origin and local microenvironment and identify several potential regulators from TF-binding motifs within these regions. We further assess the essential contribution of tissue environment by replacing endogenous macrophages with adult bone-marrow-derived cells and transferring differentiated macrophages into a new tissue microenvironment. Collectively, our results indicate that, aside from ontogeny, the environment plays a critical role in shaping the unique identity and function of tissue-resident macrophages through the regulation of TFs.

RESULTS

Genome-wide Assays to Identify Regulatory Elements in Macrophages

To elucidate the transcriptional and epigenomic networks in tissue-resident macrophages, we performed an array of complementary genome-wide assays on at least two biological replicates followed by high-throughput sequencing: RNA-seq, chromatin immunoprecipitation (ChIP-seq), and an assay for transposase-accessible chromatin (ATAC-seq) (Figure 1A). We purified macrophages, monocytes, and neutrophils from fresh mouse tissues using fluorescence-activated cell sorting (FACS) (Experimental Procedures). Global gene expression profiles of purified cells were obtained by RNA-seq, and cells intended for ChIP-seq were crosslinked upon single-cell suspension, prior to sorting, to minimize the impact on chromatin state. Cross-linked samples of each population were used for profiling histone modifications, such as H3K4me1 (candidate enhancers), H3K4me2 (promoters and enhancers), H3K4me3 (promoters), and H3K27ac (active enhancers). Finally, we identified open chromatin regions through ATAC-seq (Buenrostro et al., 2013; Lara-Astiaso et al., 2014).

Tissue-Resident Macrophages Can Be Distinguished by Their Gene Expression Patterns

To probe the spectrum of gene expression profiles among tissue-resident macrophages, we examined seven macrophage populations (brain microglia, spleen red pulp macrophages, liver Kupffer cells, lung macrophages, peritoneal cavity macrophages, and colonic large and ileal small intestinal macrophages), as well as monocytes. We identified 3,348 genes that were differentially expressed between at least two tissue-resident macrophages or monocytes (Figure 1B and Table S1). Many genes coding for TFs were uniquely expressed in specific macrophage populations, including *Sall1* in microglia and *Spi-c* in red pulp macrophages (Figures 1B and 1C). Other population-specific genes included *Clec4f* in Kupffer cells (Yang et al., 2013), *Car4* in lung macrophages, and *Tgfb2* in peritoneal macrophages (Figure 1C). Differentially expressed genes clustered into 11 groups by their expression patterns across samples (Figure 1B). Interestingly, macrophages that are presumably exposed to similar environmental cues displayed similar patterns of expression (Figures 1B, S1B, and S1C available online). Kupffer cells and splenic macrophages shared a cluster of highly expressed genes that are enriched for gene ontology (GO) annotations, such as heme and porphyrin metabolic processes, indicating their active role in erythrocyte turnover (Figures 1B and S1A, cluster III) (Chow et al., 2013). Similarly, small and large intestinal macrophages both express genes enriched for GO annotations that likely reflect their microbiota-exposed environment, such as response to bacterium and antigen processing (Figures 1B and S1A, cluster VII). RNA-seq analysis identified many genes expressed differentially by tissue-resident macrophage populations and monocytes and thereby corroborates and extends earlier expression profiling studies highlighting the inherent plasticity of this immune cell type (Gautier et al., 2012b).

Unique Regulatory Elements Distinguish Myeloid Cells

Profiling genome-wide histone modifications can shed light on the current regulatory state of a cell type. We focused on the distributions of H3K4me3, H3K4me1, and H3K27ac because, taken together, these marks classify three important functional elements: promoters, poised enhancers, and active enhancers. To better understand the mechanisms underlying macrophage plasticity, we compared the histone modification signal of circulating myeloid cells, specifically monocytes and neutrophils, to an average macrophage signature obtained by computationally merging all macrophage populations (Figure 2A). The promoter of *Mertk* is active in macrophages, but not monocytes or neutrophils as visualized by the “merged” macrophage H3K4me3 signal (Figure 2A). However, the majority of active promoters—regions with high H3K4me3 intensity—were shared by all myeloid cells (8,861 of 10,806 promoters, 82%; Figures 2B and S2B and Table S2A). On the other hand, of the total 30,976 putative enhancers, defined as regions distal to the transcriptional start site (TSS) with high H3K4me1 and low H3K4me3, only 8,260 (27%) were shared by macrophages, monocytes, and neutrophils. Indeed, both the loci of *Emr1* (F4/80) and *Mertk* feature intragenic enhancers unique to macrophages (Figures 2A and S2E). Active enhancers marked with H3K27ac were even less likely to be shared between all three myeloid cell types (10%; Figure S2A). For instance, the gene locus harboring the complement system genes (*C1qa*) contains a macrophage-specific H3K27ac-enriched region (Figures 2A and S2E). Macrophage-specific enhancers were less conserved than other

myeloid enhancers, suggesting that they are a late-acquired evolutionary function (Figure S2D). Interestingly, of the 12,743 (7,825 active) macrophage-specific enhancers, relatively few (< 2%) are shared across all macrophage populations (Figure S2C). Because enhancer usage is highly differential across cell types when compared to promoters, the enhancer landscapes likely form the basis for macrophage specificity and plasticity.

To identify candidate regulators responsible for the distinct enhancer landscape of macrophages, monocytes, and neutrophils, we assessed these regions for enriched motifs and matched them to differentially expressed TFs (Table S2B). The TF-binding motif of PU.1 was common in all enhancer regions and was overrepresented in H3K4me1-marked regions shared by all ($p = 10^{-6}$) myeloid cell types (Figure 2C). Cell-type-specific enhancers, on the other hand, tend to be bound by specific sets of TFs that regulate their chromatin states (Ghisletti et al., 2010; Heinz et al., 2010; Lara-Astiaso et al., 2014; Winter and Amit, 2014). Macrophage-specific enhancer regions exhibited significant overrepresentation of the Maf motif ($p = 10^{-23}$), in addition to high and specific expression of *Mafb* and *Maf* (Figures 2D and S2F), TFs known for their role in driving terminal macrophage differentiation (Aziz et al., 2009). Consistent with previous reports of *Klf4* as a monocyte regulator (Feinberg et al., 2007), enhancer regions unique to monocytes were enriched for the *Klf* motif ($p = 10^{-6}$), and *Klf4* was highly expressed in monocytes (Figures 2D and S2G). Finally, the *Cebp* motif was highly overrepresented in neutrophil-specific enhancers ($p = 10^{-30}$; Figure 2D). Of the *Cebp* family members implicated in myeloid cell differentiation, *Cebpe* is specifically required for neutrophil development (Yamanaka et al., 1997), and *Cebpe* is highly expressed in neutrophils (Figures 2D and S2H). Collectively, macrophages, monocytes, and neutrophils display highly distinct chromatin landscapes, despite their common lineage, indicating that the epigenome contributes significantly to cell-type specificity among myeloid cells.

Tissue-Resident Macrophages Exhibit Distinct Enhancer Landscapes that Reflect Ontogeny and Microenvironment

Because of the high divergence in tissue-resident macrophage expression and function, we next analyzed the chromatin landscape within the macrophage cell type. To determine the spectrum of enhancer usage across macrophage populations, we compared the chromatin profile of the 30,976 defined myeloid enhancers. We established that the vast majority of macrophage enhancers are unique to a small subset of populations (Figures 3 and 4). When we calculated the pairwise correlations of H3K4me1 read density between all samples, we found that the macro-phage populations were more similar to each other than to neutrophils. However, the H3K4me1-marked enhancers in different macrophage populations display a high level of variation, especially when compared with H3K4me3 promoter signal (Figure 4A). The reproducibility and tissue specificity of macrophage enhancers were verified by biological replicates (mean $r = 0.885$). Moreover, another mark of enhancer usage, H3K4me2, uniquely predicted H3K4me1-marked regions within a sample with high accuracy (Figure S3D). This variation is representative of the distinct set of enhancers utilized by individual macrophage populations (Figures 4A and 4B).

Indeed, when the catalog of enhancers was clustered by H3K4me1 intensity across the populations, nearly all tissue-resident macrophages demonstrated uniquely utilized enhancers (Figure 4B, clusters I–III, V, VIII, and X). For instance, the intergenic region of *Sall1* exhibited a microglia-specific region enriched for H3K4me1 (cluster I; Figure 3A). Enhancers unique to lung macrophages were enriched for genes involved in metabolism of lipids and lipoproteins, indicating the role of these cells in surfactant lipoprotein metabolism (Hussell and Bell, 2014) (Table S3, cluster VIII). Moreover, an H3K4me1-marked region exclusive to peritoneal macrophages was detected within the *Gata6* gene locus (cluster X; Figure 3A). The highly similar small and large intestinal macrophages shared enhancers utilized in no other populations, including the regions adjacent to *Runx3* (cluster XI; Figure 3A). In confirmation, these clusters were reproduced by H3K4me2 intensity in the same regions, which was highly correlated with H3K4me1 across all analyzed macrophage populations (Figures S3A and S3B). In general, unique macrophage clusters are associated with tissue-specific genes and related functions (Table S3), indicating a potential role for the microenvironment in shaping chromatin dynamics.

Hierarchical clustering based on H3K4me1-marked or H3K4me2-marked enhancers positioned the monocytes next to the junction of small and large intestinal macrophages (Figures 4C and Figure S3C). This suggests that ontogenic relationships influence chromatin dynamics because intestinal macrophages, as opposed to the other tissue-resident macrophages analyzed, are mostly monocyte derived (Bain et al., 2014; Bogunovic et al., 2009; Varol et al., 2009). Accordingly, many more monocyte enhancers remain open in intestinal macrophages (85% and 87%) compared to other tissue-resident macrophages (chisquare $p < 10^{-5}$; Figure 4D). Conversely, embryo-derived macrophages shared many enhancers that are not present in intestinal macrophages or monocytes, including enhancers close to *Rxra* and *Marco* (Figure 4B, cluster XVII).

Analysis of the enhancer landscape also exposes relationships among tissue-resident macrophages that are unrelated to ontogeny. For instance, Kupffer cells and spleen macrophages cluster together as a result of the many enhancers they share (cluster IV, Figure 4C), likely reflecting the impact of their similar environments characterized by prominent erythrocyte exposure. In addition, microglia and lung macrophages are most distant from other macrophages in the hierarchical tree and are excluded from an enhancer cluster shared by all other populations (cluster XV, Figure 4C).

Collectively, the distinct enhancer usage of different tissue-resident macrophages highlights how chromatin state dynamics allow for plasticity within a given cell type. Although some patterns reflect development, the level of variability between macrophage populations extends beyond this dimension. Thus, ontogeny, together with local microenvironment, likely contributes to shaping the enhancer landscape of tissue-resident macrophages.

Poised Enhancers Reflect Both Developmental Origin and Tissue Specificity

H3K4me1-marked enhancers are considered either active or poised, as demarcated by the presence or absence of the H3K27ac mark (Creyghton et al., 2010). To further explore enhancer activity, we analyzed the distribution of H3K27ac in H3K4me1-marked enhancers (Figure S4). For example, the enhancer regions in the *Itgax* locus encoding the integrin

CD11c are marked with H3K4me1 in all macrophages, although expression of *Itgax* is restricted to lung and intestinal macrophages. This is reflected in the H3K27ac signal denoting transcriptional activity in only these macrophage populations (Figures 3B and 3C). Likewise, *Cx3cr1*, a gene encoding a chemokine receptor, exhibits a H3K4me1-marked region shared by all macrophages but is activated only in intestinal macrophages and microglia (Figures 3B and 3C). On the other hand, the region surrounding the *Vcam1* gene, along with the previously described loci (Figure S4A), exhibits tissue-specific macrophage enhancers with H3K4me1 signal in proportion to its H3K27ac activity and expression (Figures 3B and 3C). Thus, analysis of both H3K4me1 and H3K27ac in enhancers allows us to describe the current activity, developmental origin, and potential of these cells to activate various gene sets under external stimuli.

We determine enhancer activity based on the level of H3K27ac intensity in H3K4me1-marked candidate enhancers and classify poised enhancers as those that have low H3K27ac in all populations (Experimental Procedures). On a global scale, H3K27ac intensity correlates with H3K4me1 in enhancers and exhibits similar relationships between populations (Figures S4B–S4E). However, individual enhancers vary in the relationship between the two marks as evidenced by differing proportions of active and poised enhancers in the H3K4me1 clusters (Figure 4B, right bar). Dissecting this pattern further, we find that enhancers shared by multiple macrophage populations have a higher level of activity than those that are shared by few or none (Figure 4E). For instance, enhancers that were present in all but one of the populations were significantly more likely to be active in Kupffer cells than those enhancers shared with only one other population (kstest $p = 9.35 \times 10^{-37}$; Figure 4E). This trend held true for all samples except neutrophils (Figure S4F). Therefore, plasticity of tissue-resident macrophages may arise from selective activation of developmentally derived enhancers or de novo enhancers triggered by the local microenvironment.

Tissue Regulators Define Distinct Sets of Macrophage Enhancers

We hypothesized that the distinct enhancer landscape in tissue-resident macrophages is the result of the combinatorial action of tissue regulators. Assuming that the expression of TFs should match the utilization of the enhancers that they regulate, we established a computational pipeline to identify candidate regulators for each enhancer cluster (Figure 5A). Because H3K4me1-marked enhancers may span several kilobases, but TF motifs usually occupy no more than a dozen bases, we generated ATAC-seq peaks corresponding to the same tissue-resident macrophages to narrow our search regions to the likely site of TF binding (Buenrostro et al., 2013; Lara-Astiaso et al., 2014). Marking open chromatin, ATAC-seq intensity is highly correlated with H3K4me1 intensity in enhancers, and the vast majority of putative enhancer regions contain at least one ATAC-seq peak (Figures 5B, S5C, and S5D). For each cluster, we overlapped the enhancer coordinates with the ATAC-seq peak and lifted the DNA sequence from these regions to search for significantly enriched, cluster-specific motifs. Finally, to determine the most likely regulator from the TF family that matched the motif, we compared the gene expression profile of all family members to the enhancer signature. In this manner, we identified candidate regulators for many of the clusters shown in Figure 4B (Figures 5C–5E, S5E, and S5F and Table S4).

For example, we found that the GATA motif was overrepresented in the cluster of enhancers specific to peritoneal macrophages (cluster X). Among the GATA TF family members, *Gata6* was the most highly and differentially expressed in peritoneal macrophages (Figures 5C–5E). Therefore, *Gata6* is a likely regulator of peritoneal-specific macrophage enhancers, as supported by recently published results (Gautier et al., 2014; Okabe and Medzhitov, 2014; Rosas et al., 2014). Indeed, GATA motifs appear within enhancers associated with genes expressed exclusively in peritoneal macrophages, such as *Tgfb2* (Figures 1A and 5C). Likewise, MEF2 binding motifs were overrepresented in microglia-specific enhancer clusters and appeared at enhancers of microglia-specific genes such as *Fcrls* (Figures 5C, 5D, and 4B, clusters I and II). *Mef2c* was implicated as the mostly highly and differentially expressed MEF2 family member in microglia (Figures 5C–5E and Table S4). Other candidate TFs include *Lxra* in Kupffer cells and spleen macrophages (clusters III and V) and *Pparg* in spleen and lung macrophages (clusters V and VI). Intestinal macrophages, along with monocytes and neutrophils, are enriched for RUNX family motifs, with *Runx3* highly expressed in intestinal macrophages (clusters XI–XIV) (Figures 5D and 5E and Table S4).

Our data suggest that the distinct enhancer landscapes of tissue-resident macrophages result from the restricted expression and binding of TFs. The orchestration of chromatin modifications is regulated by crosstalk between the environment and ontogeny through a small number of TFs (Heinz et al., 2010). Hence, macrophage identity is shaped by tissue-restricted TFs in conjunction with those ubiquitously present in macrophages, such as PU.1.

Macrophage Enhancer Landscapes Are Imparted by the Microenvironment

To assess the contribution of environmental signals as opposed to developmental processes, we assessed the chromatin state of macrophages derived from transplanted adult bone marrow (BM) that replace endogenous embryo-derived tissue-resident macrophages upon lethal irradiation (Ginhoux et al., 2010; Hashimoto et al., 2013; Schulz et al., 2012; Virolainen, 1968; Yona et al., 2013) (Figure 6A). Four months after engraftment, we retrieved the donor transplant-derived lung, spleen, liver, and peritoneal macrophages using the congenic CD45 alleles to distinguish them from host macrophages (Figure S6A; Experimental Procedures). Critically, we found that macrophages from transplanted adult BM acquire enhancers found in embryonic macrophages in a tissue-specific manner, including those in the *Car4* locus of lung macrophages and the *Gata6* locus found in peritoneal macrophages (Figure 6B).

Importantly, the H3K4me1 intensity of adult transplant-derived macrophages was highly reproducible and much more similar to their embryo-derived counterpart than any other macrophage population (Figures 6C, 6D, and S6B–S6D). Macrophages derived from donor BM recovered 89%–98% overall and 47%–92% of tissue-specific enhancers from the reference (Figure 6E, Experimental Procedures). Similarly, principal component analysis (PCA) revealed that transplanted macrophages were positioned closer to their corresponding reference macrophage than other reference or transplanted macrophages (Figure 6F). Similar results were seen with active enhancer (H3K27ac) regions (Figures S6E–S6H). Collectively, these data establish that adult bone marrow precursors can acquire the tissue-specific enhancer landscape of macrophages seeded in the tissues during development, reinforcing

that the tissue microenvironment plays a prominent and active role in establishing macrophage identity.

Differentiated Tissue-Resident Macrophages Can Be Reprogrammed by the Tissue Microenvironment

Typically, once the chromatin landscape is specified during differentiation, cells lose the plasticity to revert to their original precursor state or convert — without artificial manipulation — into other cell types. Based on the results of the above transplant experiment, we asked whether differentiated tissue-resident macrophages would retain sufficient plasticity to adapt to a new microenvironment upon transfer into an ectopic tissue.

Lung and peritoneal macrophages display distinct expression profiles (Figure 7A). Moreover, they harbor distinct chromatin landscapes with tissue-specific enhancers and candidate regulators, such as *Gata6* and *Pparg* (Figures 7B, 7C, 5E, and S7A). To test the potential of the environment to reprogram differentiated macrophages, we sorted peritoneal macrophages from CD45.1⁺ donor mice and transferred them intratracheally into the alveolar cavity of CD45.2⁺ animals (Figures 7D and S7B).

Although the engrafted macrophages retained high levels of CD11b surface expression, akin to endogenous peritoneal macrophages, ICAM2 — a peritoneal macrophage-specific surface marker (Gautier et al., 2012b) (Figure 7A) — was downregulated upon transfer to levels on par with lung macrophages (Figure 7E). Transferred macrophages upregulated lung macrophage-specific genes, including *Chi3l3*, *Sftpc*, *Car4*, and the TF *Pparg* (Figure 7F), while downregulating peritoneal macrophage-specific genes, including *Alox15* and the TF *Gata6* (Figure 7F). Global RNA-seq analysis of transferred cells demonstrated that 70% of genes highly and differentially expressed in peritoneal or lung macrophages (708 of 1,014) had switched from a peritoneal cavity profile to resemble lung macrophages (Figure 7G and Table S5), resulting in a significant shift in the distribution of genes ($p = 5.8 \times 10^{-37}$; $p = 2.9 \times 10^{-37}$; Figure S7C). The overall transition was confirmed by PCA analysis of the expression profiles, which placed transferred cells closer to lung than peritoneal macrophages (Figure 7H). This transfer experiment indicates that differentiated tissue-resident macrophages retain their plasticity and further emphasizes the critical role of the microenvironment in shaping the functional identity of steady-state macrophages.

DISCUSSION

The epigenomic state of a cell regulates gene expression, differentiation, and cellular identity. We show that, at least in the case of tissue-resident macrophages, the chromatin landscape provides a mechanism for plasticity and allows for crosstalk between the environment and tissue-specific macrophage function. We provide a comprehensive resource of the annotated regulatory elements, including promoters (H3K4me3), poised enhancers (H3K4me1), and active enhancers (H3K27ac) of seven different tissue-resident macrophage populations, as well as monocytes and neutrophils. We demonstrate that tissue-resident macrophage populations are distinct with respect to their set of regulatory elements. Much of the previous work on macrophage chromatin states explored either BM culture-derived macrophages or thioglycollate-elicited monocyte-derived peritoneal macrophages.

Although these studies offered many insights on general macrophage function, our results show that the application of these earlier findings to all macrophage populations cannot be taken for granted. Rather, tissue-resident macrophages are subject to an additional level of regulation by a combination of ontogeny and the dynamic influence of the tissue microenvironment, which together shape their distinct chromatin landscapes.

Tissue-resident macrophages have distinct global expression profiles, as we show using RNA-seq in confirmation of prior results obtained on a smaller scale (Gautier et al., 2012b). To assess the extent of artificial induction of stimulus-response genes in our RNA-seq data, we compared the expression profiles of the tissue-resident macrophage populations with stimulated dendritic cells across multiple time points (Garber et al., 2012). Because the highest correlation was with unstimulated cells, we conclude that our protocols did not cause undue activation of immediate early genes (Figure S2D). Chromatin states, moreover, are stable within the time span of macrophage isolation (Experimental Procedures) (Garber et al., 2012; Ostuni et al., 2013); thus, the *in vivo* chromatin states are even less likely to be disrupted.

Through assessing enhancer activity, we add a new dimension to understanding how the identities of tissue-resident macrophages are regulated. Some poised enhancers are inherited in development and thus encode ontogenic memory (Nord et al., 2013); such enhancers are ubiquitously marked with H3K4me1 but may be active only in a subset of populations (Sternik et al., 2013). Lineage-tracing experiments show that *Cx3cr1*, which displays a poised enhancer already at the common myeloid precursor (CMP) stage (Lara-Astiaso et al., 2014), is expressed during development of all macrophage populations (Yona et al., 2013). Interestingly, the *Cx3cr1* locus retains H3K4me1-marked enhancers in all tissue-resident macrophages populations, although it is almost exclusively acetylated and expressed in microglia and intestinal macrophages. *De novo* enhancers encompass much of the diversity between different tissue-resident macrophage populations and provide a possible account for macrophage plasticity. Many of these regions are poised and, along with latent enhancers not preemptively marked for activation, reflect the potential to respond to future stimuli (Ostuni et al., 2013). Indeed, we show that the highest percentages of poised enhancers are at regions present in only one or two macrophage populations, demonstrating complex regulatory mechanisms, which can only be analyzed comprehensively on the level of the chromatin.

Master regulators, such as PU.1, work in combination with other TFs to specify active regulatory regions in a cell-type-specific manner (Heinz et al., 2010). Here, we implicate Maf family TFs, such as Maf and MafB, in the establishment of macrophage-specific regulatory regions. Within macrophages, we further identified candidate regulators that may work in combination to establish the distinct chromatin landscape for each tissue-resident macrophage population. These TFs, which include Mef2c in microglia (Speliotes et al., 1996), Lxra in Kupffer cells and splenic macrophages (A-Gonzalez et al., 2013; Joseph et al., 2004), Pparg in splenic red pulp and lung macrophages (Gautier et al., 2012a; Schneider et al., 2014), Gata6 in peritoneal macrophages (Okabe and Medzhitov, 2014), and Runx3 in intestinal macrophages, have varying support in the literature. Future studies should focus on knocking out or overexpressing these candidate regulators and observing the effects on

the regulatory networks, epigenomic landscape, and identity of specific macrophage populations.

These candidate regulators are likely to be the conduit through which signals in the tissue microenvironment influence the chromatin landscape of macrophages. Our results are consistent with previous studies showing that heme and retinoic acid promote the induction of the tissue-specific macrophage TFs, Spi-C and Gata6, respectively (Haldar et al., 2014; Okabe and Medzhitov, 2014). Notably, some of the TFs we identified, such as Klf4 and Pparg, have been reported to be associated with functional macrophage polarization (Murray et al., 2014). However, given the heterogeneity of enhancer landscapes and the tissue-specific signatures of poised enhancers, the activation of tissue-resident macrophages is likely to be more complex than previously anticipated. We confirmed the role of the environment in shaping macrophage identity by enforcing replacement of endogenous, embryo-derived macrophages with adult BM cells, and almost all enhancers were recovered in a tissue-specific manner. The question of whether monocytes contribute to the embryo-derived macrophage population in the case of nonirradiating injury or infection in the long-term remains unresolved (Epelman et al., 2014; Ginhoux and Jung, 2014). However, our study indicates that, if precursors do enter and remain in the tissue, they will be able to assimilate to the local macrophage population. Moreover, they adopt both poised and active regulatory elements, indicating their functionality.

Interestingly, when we transferred fully differentiated macrophages to an alternate tissue, we found that the new environment was sufficient to reshape their expression. The chromatin landscape is, therefore, specialized within the tissue, while still retaining the capacity to be reversed (as seen in Okabe and Medzhitov, 2014) and reprogrammed. This also presents the possibility that peritoneal macrophages, or other differentiated macrophages, could potentially serve as a therapeutic source of macrophages, as recently shown for precursors (Happle et al., 2014; Suzuki et al., 2014).

Macrophages are important sentinels of the immune system, embedded in each tissue, and are responsive to local changes in the microenvironment. Identifying the regulatory elements that define each tissue-resident macrophage identity is, therefore, critical for understanding their role in alerting the immune system to disease. The means by which the dysregulation of chromatin landscape and transcription factors can lead to impaired function directs the exploration of new therapeutic strategies to stimulate or inhibit the appropriate, tissue-specific macrophage response. Finally, a similar study in humans will be highly beneficial for uncovering the mechanisms of regulatory aberrations in immunological disorders.

EXPERIMENTAL PROCEDURES

Mice

C57BL/6 mice were purchased from Harlan (Rehovot, Israel). Macrophages were isolated from 6- to 7-week-old females. All animals were kept in specific pathogen-free (SPF) conditions and handled according to the protocols approved by the Weizmann Institute Animal Care Committee as per international guidelines.

Tissue Processing, Flow Cytometry, and Cell Sorting

Macrophages were purified following protocols (Extended Experimental Procedures; Data S1) as previously described (Gautier et al., 2012b; Zigmond et al., 2012). Cells were isolated directly from mouse tissue, stained, and sorted on an Aria III either into lysis/binding buffer (Life Technologies) for RNA-sequencing or crosslinked in 1% formaldehyde (Pierce Biotechnologies) prior to sorting into PBS for ChIP-seq.

Bone Marrow Transplant and Intratracheal Transfer

Cells were isolated from CD45.1 mice by bone marrow flushing and injected IV into irradiated 6-week-old CD45.2 females. Macrophages were isolated from tissues and processed as above 11–12 weeks later. For intratracheal transfer, peritoneal cavity macrophages were sorted from CD45.1 animals. 5×10^5 cells in sterile PBS or PBS alone were placed in the distal oral cavity of anesthetized 5-week-old animals. Cells were isolated after 15 days from the lung and processed as above.

Quantitative PCR

mRNA was isolated with Dynabeads oligo(dT) (Life technologies), and reverse-transcribed to cDNA using AffinityScript RT kit (Agilent). Quantitative PCR (qPCR) was performed with LightCycler480 SYBR Green I Master Mix (Roche) in triplicate, normalizing to Actb. Primers are listed in Table S6.

RNA Isolation, Library Construction, and Analysis

10^4 - 10^5 cells from each population were sorted into 100–200 ml of lysis/binding buffer (Life Technologies). mRNA was captured with 12 ml of Dynabeads oli-go(dT) (Life Technologies), washed, and eluted at 70°C with 10 ml of 10 mM Tris-Cl (pH 7.5). We used a derivation of MARS-seq as described (Jaitin et al., 2014), developed for single-cell RNA-seq to produce expression libraries with a minimum of two replicates per population. Table S7 shows MARS-seq primers. We sequenced an average of 4 million reads per library and aligned them to the mouse reference genome (NCBI 37, mm9) using TopHat v2.0.10 (Trapnell et al., 2009) with default parameters. Expression levels were calculated and normalized using ESAT software (<http://garberlab.umassmed.edu/software/esat>). RNA-seq analysis in Figure 1 focused on genes in 25th percentile of expression with a 2-fold differential between at least two populations. For transferred macrophages in Figures 7G and 7H, highly expressed and differential (2-fold) peritoneum and lung macrophage genes were analyzed. Details are provided in the Extended Experimental Procedures.

High-Throughput-ChIP-Seq

10^5 crosslinked cells were used for ChIP-seq, as described (Blecher-Gonen et al., 2013; Garber et al., 2012). Following crosslinking and sorting, chromatin was fragmented by sonication, and the mixture was purified with magnetic beads (Invitrogen, Dynabeads) conjugated to 1 ng of H3K4Me1 (Abcam and Millipore), H3K4Me2 (Abcam), H3K4Me3 (Millipore), or H3K27Ac (Abcam) antibodies. After barcoding, pooled DNA was sequenced (HiSeq 1500, Illumina) to achieve a minimum of 10^7 aligned reads per sample.

ATAC-Seq

To profile open chromatin, we used the ATAC-seq protocol developed by Buenrostro et al. (2013) with modifications described in the Extended Experimental Procedures and by Lara-Astiaso et al. (2014).

Processing of ChIP-Seq, ATAC-Seq, and Chromatin Peak Calling

Reads were aligned to the mouse reference genome (mm9, NCBI 37) using Bowtie aligner version 1.0.0 (Langmead et al., 2009) with best match parameters (bowtie -m 1-sam-best-strata -v 2). To identify regions of enrichment, peaks, from ChIP-seq reads of H3K4me1 and H3K4me3, we used the HOMER package *makeTagDirectory* followed by *findPeaks* command with the histone parameter (Heinz et al., 2010). Union peaks file were generated by combining and merging overlapping peaks in all samples.

Chromatin Analysis

The read density (number of reads in 10 million total reads per 1,000 bp) was calculated in each region from union peaks files for H3K4me1 and H3K4me3. We quantile normalized the average read density of replicates in high-confidence regions (i.e., above threshold in both replicates; Extended Experimental Procedures and Data S1) of each cell type. The region intensity was given in log-base2 of the normalized density ($\log_2(x+1)$). We define promoters as these 10,806 H3K4me3 regions and enhancers as the 30,976 H3K4me1 nonpromoter regions — i.e., neither overlapping H3K4me3 regions nor within $\pm 2,000$ bp of a TSS (Data S1). We calculated intensity of H3K27ac in each H3K4me1 region designated as an enhancer. To compare the relative activity of clusters, we classified 14,112 active enhancers as those that had density ≥ 15 before normalization (see below) in any cell type (Data S1). Details are provided in the Extended Procedures.

For motif finding, we independently called peaks in ATAC-seq, as above, and identified the maximum peak that overlapped each enhancer region. The overlapping sequences were input for HOMER package motif finder algorithm *findMotifGenome.pl* (Heinz et al., 2010). See also Extended Experimental Procedures.

Gene Tracks and Normalization

All gene tracks were visualized as *bigWig* files of the combined replicates normalized to 10,000,000 reads. The merged macrophage track was created by adding together the fastq reads of all macrophage populations and normalizing to total reads. For visualization, the tracks were smoothed by averaging over a sliding window of 500 bases.

Supplementary Material

Refer to Web version on PubMed Central for supplementary material.

ACKNOWLEDGMENTS

We thank members of the I.A., S.J., and M.M. labs for discussions. We thank Tali Wiesel and Genia Brodsky for artwork. Research in the I.A. lab is supported by the European Research Council (309788) and the Israeli Science Foundation (1782/11), The Human Frontiers Science Program, Career Development Award, and the Center for

Excellence in Genome Science from the NHGRI 1P50HG006193. Research in the S.J. lab is supported by the Israeli Science Foundation (887/11), the European Research Council (340345), and the Deutsche Forschungsgemeinschaft (FOR1336). M.M. is supported by NIH R01CA154947A, NIHR01CA173861, NIHU01AI095611, and NIH-R01AI104848. D.W. is grateful to the Azrieli Foundation for the Azrieli Fellowship award and EMBO for the Long-Term Fellowship. Y.L. is grateful for the MSTP training grant support.

REFERENCES

- A-Gonzalez N, Guillen JA, Gallardo G, Diaz M, de la Rosa JV, Hernandez IH, Casanova-Acebes M, Lopez F, Tabraue C, Beceiro S, et al. The nuclear receptor LXR α controls the functional specialization of splenic macrophages. *Nat. Immunol.* 2013; 14:831–839. [PubMed: 23770640]
- Abutbul S, Shapiro J, Szaingurten-Solodkin I, Levy N, Carmy Y, Baron R, Jung S, Monsonego A. TGF- β signaling through SMAD2/3 induces the quiescent microglial phenotype within the CNS environment. *Glia.* 2012; 60:1160–1171. [PubMed: 22511296]
- Aziz A, Soucie E, Sarrazin S, Sieweke MH. MafB/c-Maf deficiency enables self-renewal of differentiated functional macrophages. *Science.* 2009; 326:867–871. [PubMed: 19892988]
- Bain CC, Bravo-Blas A, Scott CL, Gomez Perdiguero E, Geissmann F, Henri S, Malissen B, Osborne LC, Artis D, Mowat AM. Constant replenishment from circulating monocytes maintains the macrophage pool in the intestine of adult mice. *Nat. Immunol.* 2014; 15:929–937. [PubMed: 25151491]
- Blecher-Gonen R, Barnett-Itzhaki Z, Jaitin D, Amann-Zalcenstein D, Lara-Astiaso D, Amit I. High-throughput chromatin immunoprecipitation for genome-wide mapping of in vivo protein-DNA interactions and epigenomic states. *Nat. Protoc.* 2013; 8:539–554. [PubMed: 23429716]
- Bogunovic M, Ginhoux F, Helft J, Shang L, Hashimoto D, Greter M, Liu K, Jakubzick C, Ingersoll MA, Leboeuf M, et al. Origin of the lamina propria dendritic cell network. *Immunity.* 2009; 31:513–525. [PubMed: 19733489]
- Buenrostro JD, Giresi PG, Zaba LC, Chang HY, Greenleaf WJ. Transposition of native chromatin for fast and sensitive epigenomic profiling of open chromatin, DNA-binding proteins and nucleosome position. *Nat. Methods.* 2013; 10:1213–1218. [PubMed: 24097267]
- Butovsky O, Jedrychowski MP, Moore CS, Cialic R, Lanser AJ, Gabriely G, Koeglsperger T, Dake B, Wu PM, Doykan CE, et al. Identification of a unique TGF- β -dependent molecular and functional signature in microglia. *Nat. Neurosci.* 2014; 17:131–143. [PubMed: 24316888]
- Chow A, Huggins M, Ahmed J, Hashimoto D, Lucas D, Kunisaki Y, Pinho S, Leboeuf M, Noizat C, van Rooijen N, et al. CD169⁺ macrophages provide a niche promoting erythropoiesis under homeostasis and stress. *Nat. Med.* 2013; 19:429–436. [PubMed: 23502962]
- Cirillo LA, Lin FR, Cuesta I, Friedman D, Jarnik M, Zaret KS. Opening of compacted chromatin by early developmental transcription factors HNF3 (FoxA) and GATA-4. *Mol. Cell.* 2002; 9:279–289. [PubMed: 11864602]
- Creyghton MP, Cheng AW, Welstead GG, Kooistra T, Carey BW, Steine EJ, Hanna J, Lodato MA, Frampton GM, Sharp PA, et al. Histone H3K27ac separates active from poised enhancers and predicts developmental state. *Proc. Natl. Acad. Sci. USA.* 2010; 107:21931–21936. [PubMed: 21106759]
- Epelman S, Lavine KJ, Randolph GJ. Origin and functions of tissue macrophages. *Immunity.* 2014; 41:21–35. [PubMed: 25035951]
- Ernst J, Kheradpour P, Mikkelson TS, Shores N, Ward LD, Epstein CB, Zhang X, Wang L, Issner R, Coyne M, et al. Mapping and analysis of chromatin state dynamics in nine human cell types. *Nature.* 2011; 473:43–49. [PubMed: 21441907]
- Feinberg MW, Wara AK, Cao Z, Lebedeva MA, Rosenbauer F, Iwasaki H, Hirai H, Katz JP, Haspel RL, Gray S, et al. The Kruppel-like factor KLF4 is a critical regulator of monocyte differentiation. *EMBO J.* 2007; 26:4138–4148. [PubMed: 17762869]
- Felsenfeld G, Groudine M. Controlling the double helix. *Nature.* 2003; 421:448–453. [PubMed: 12540921]
- Garber M, Yosef N, Goren A, Raychowdhury R, Thielke A, Guttman M, Robinson J, Minie B, Chevrier N, Itzhaki Z, et al. A high-throughput chromatin immunoprecipitation approach reveals

principles of dynamic gene regulation in mammals. *Mol. Cell.* 2012; 47:810–822. [PubMed: 22940246]

- Gautier EL, Chow A, Spanbroek R, Marcelin G, Greter M, Jakubzick C, Bogunovic M, Leboeuf M, van Rooijen N, Habenicht AJ, et al. Systemic analysis of PPAR γ in mouse macrophage populations reveals marked diversity in expression with critical roles in resolution of inflammation and airway immunity. *J. Immunol.* 2012a; 189:2614–2624. [PubMed: 22855714]
- Gautier EL, Shay T, Miller J, Greter M, Jakubzick C, Ivanov S, Helft J, Chow A, Elpek KG, Gordonov S, et al. Immunological Genome Consortium. Gene-expression profiles and transcriptional regulatory pathways that underlie the identity and diversity of mouse tissue macrophages. *Nat. Immunol.* 2012b; 13:1118–1128. [PubMed: 23023392]
- Gautier EL, Ivanov S, Williams JW, Huang SC, Marcelin G, Fairfax K, Wang PL, Francis JS, Leone P, Wilson DB, et al. Gata6 regulates aspartoacylase expression in resident peritoneal macrophages and controls their survival. *J. Exp. Med.* 2014; 211:1525–1531. [PubMed: 25024137]
- Ghisletti S, Barozzi I, Mietton F, Polletti S, De Santa F, Venturini E, Gregory L, Lonie L, Chew A, Wei C-L, et al. Identification and characterization of enhancers controlling the inflammatory gene expression program in macrophages. *Immunity.* 2010; 32:317–328. [PubMed: 20206554]
- Ginhoux F, Jung S. Monocytes and macrophages: developmental pathways and tissue homeostasis. *Nat. Rev. Immunol.* 2014; 14:392–404. [PubMed: 24854589]
- Ginhoux F, Greter M, Leboeuf M, Nandi S, See P, Gokhan S, Mehler MF, Conway SJ, Ng LG, Stanley ER, et al. Fate mapping analysis reveals that adult microglia derive from primitive macrophages. *Science.* 2010; 330:841–845. [PubMed: 20966214]
- Gross DS, Garrard WT. Nuclease hypersensitive sites in chromatin. *Annu. Rev. Biochem.* 1988; 57:159–197. [PubMed: 3052270]
- Haldar M, Kohyama M, So AY, Kc W, Wu X, Briseño CG, Satpathy AT, Kretzer NM, Arase H, Rajasekaran NS, et al. Heme-mediated SPI-C induction promotes monocyte differentiation into iron-recycling macrophages. *Cell.* 2014; 156:1223–1234. [PubMed: 24630724]
- Happle C, Lachmann N, Skuljec J, Wetzke M, Ackermann M, Brenning S, Mucci A, Jirmo AC, Groos S, Mirenska A, et al. Pulmonary transplantation of macrophage progenitors as effective and long-lasting therapy for hereditary pulmonary alveolar proteinosis. *Sci. Transl. Med.* 2014; 6:250ra113.
- Hashimoto D, Chow A, Noizat C, Teo P, Beasley MB, Leboeuf M, Becker CD, See P, Price J, Lucas D, et al. Tissue-resident macrophages self-maintain locally throughout adult life with minimal contribution from circulating monocytes. *Immunity.* 2013; 38:792–804. [PubMed: 23601688]
- Heintzman ND, Stuart RK, Hon G, Fu Y, Ching CW, Hawkins RD, Barrera LO, Van Calcar S, Qu C, Ching KA, et al. Distinct and predictive chromatin signatures of transcriptional promoters and enhancers in the human genome. *Nat. Genet.* 2007; 39:311–318. [PubMed: 17277777]
- Heintzman ND, Hon GC, Hawkins RD, Kheradpour P, Stark A, Harp LF, Ye Z, Lee LK, Stuart RK, Ching CW, et al. Histone modifications at human enhancers reflect global cell-type-specific gene expression. *Nature.* 2009; 459:108–112. [PubMed: 19295514]
- Heinz S, Benner C, Spann N, Bertolino E, Lin YC, Laslo P, Cheng JX, Murre C, Singh H, Glass CK. Simple combinations of lineage-determining transcription factors prime cisregulatory elements required for macrophage and B cell identities. *Mol. Cell.* 2010; 38:576–589. [PubMed: 20513432]
- Hussell T, Bell TJ. Alveolar macrophages: plasticity in a tissue-specific context. *Nat. Rev. Immunol.* 2014; 14:81–93. [PubMed: 24445666]
- Jaitin DA, Kenigsberg E, Keren-Shaul H, Elefant N, Paul F, Zaretsky I, Mildner A, Cohen N, Jung S, Tanay A, Amit I. Massively parallel single-cell RNA-seq for marker-free decomposition of tissues into cell types. *Science.* 2014; 343:776–779. [PubMed: 24531970]
- Joseph SB, Bradley MN, Castrillo A, Bruhn KW, Mak PA, Pei L, Hogenesch J, O’Connell RM, Cheng G, Saez E, et al. LXR-dependent gene expression is important for macrophage survival and the innate immune response. *Cell.* 2004; 119:299–309. [PubMed: 15479645]
- Kohyama M, Ise W, Edelson BT, Wilker PR, Hildner K, Mejia C, Frazier WA, Murphy TL, Murphy KM. Role for Spi-C in the development of red pulp macrophages and splenic iron homeostasis. *Nature.* 2009; 457:318–321. [PubMed: 19037245]
- Langmead B, Trapnell C, Pop M, Salzberg SL. Ultrafast and memory-efficient alignment of short DNA sequences to the human genome. *Genome Biol.* 2009; 10:R25. [PubMed: 19261174]

- Lara-Astiaso D, Weiner A, Lorenzo-Vivas E, Zaretzky I, Jaitin DA, David E, Keren-Shaul H, Mildner A, Winter D, Jung S, et al. Immunogenetics. Chromatin state dynamics during blood formation. *Science*. 2014; 345:943–949. [PubMed: 25103404]
- Laslo P, Spooner CJ, Warmflash A, Lancki DW, Lee HJ, Sciammas R, Gantner BN, Dinner AR, Singh H. Multilineage transcriptional priming and determination of alternate hematopoietic cell fates. *Cell*. 2006; 126:755–766. [PubMed: 16923394]
- Lavin Y, Merad M. Macrophages: gatekeepers of tissue integrity. *Cancer Immunol. Res.* 2013; 1:201–209. [PubMed: 24777851]
- Mortha A, Chudnovskiy A, Hashimoto D, Bogunovic M, Spencer SP, Belkaid Y, Merad M. Microbiota-dependent crosstalk between macrophages and ILC3 promotes intestinal homeostasis. *Science*. 2014; 343:1249288. [PubMed: 24625929]
- Murray PJ, Allen JE, Biswas SK, Fisher EA, Gilroy DW, Goerdt S, Gordon S, Hamilton JA, Ivashkiv LB, Lawrence T, et al. Macrophage activation and polarization: nomenclature and experimental guidelines. *Immunity*. 2014; 41:14–20. [PubMed: 25035950]
- Nord AS, Blow MJ, Attanasio C, Akiyama JA, Holt A, Hosseini R, Phouanavong S, Plajzer-Frick I, Shoukry M, Afzal V, et al. Rapid and pervasive changes in genome-wide enhancer usage during mammalian development. *Cell*. 2013; 155:1521–1531. [PubMed: 24360275]
- Okabe Y, Medzhitov R. Tissue-specific signals control reversible program of localization and functional polarization of macrophages. *Cell*. 2014; 157:832–844. [PubMed: 24792964]
- Ostuni R, Piccolo V, Barozzi I, Polletti S, Termanini A, Bonifacio S, Curina A, Prosperini E, Ghisletti S, Natoli G. Latent enhancers activated by stimulation in differentiated cells. *Cell*. 2013; 152:157–171. [PubMed: 23332752]
- Paolicelli RC, Bolasco G, Pagani F, Maggi L, Scianni M, Panzanelli P, Giustetto M, Ferreira TA, Guiducci E, Dumas L, et al. Synaptic pruning by microglia is necessary for normal brain development. *Science*. 2011; 333:1456–1458. [PubMed: 21778362]
- Rosas M, Davies LC, Giles PJ, Liao CT, Kharfan B, Stone TC, O'Donnell VB, Fraser DJ, Jones SA, Taylor PR. The transcription factor Gata6 links tissue macrophage phenotype and proliferative renewal. *Science*. 2014; 344:645–648. [PubMed: 24762537]
- Schafer DP, Lehrman EK, Kautzman AG, Koyama R, Mardinly AR, Yamasaki R, Ransohoff RM, Greenberg ME, Barres BA, Stevens B. Microglia sculpt postnatal neural circuits in an activity and complement-dependent manner. *Neuron*. 2012; 74:691–705. [PubMed: 22632727]
- Schneider C, Nobs SP, Kurrer M, Rehrauer H, Thiele C, Kopf M. Induction of the nuclear receptor PPAR- γ by the cytokine GM-CSF is critical for the differentiation of fetal monocytes into alveolar macrophages. *Nat. Immunol.* 2014; 15:1026–1037. [PubMed: 25263125]
- Schulz C, Gomez Perdiguero E, Chorro L, Szabo-Rogers H, Cagnard N, Kierdorf K, Prinz M, Wu B, Jacobsen SEW, Pollard JW, et al. A lineage of myeloid cells independent of Myb and hematopoietic stem cells. *Science*. 2012; 336:86–90. [PubMed: 22442384]
- Speliotis EK, Kowall NW, Shanti BF, Kosofsky B, Finklestein SP, Leifer D. Myocyte-specific enhancer binding factor 2C expression in gerbil brain following global cerebral ischemia. *Neuroscience*. 1996; 70:67–77. [PubMed: 8848137]
- Stergachis AB, Neph S, Reynolds A, Humbert R, Miller B, Paige SL, Vernot B, Cheng JB, Thurman RE, Sandstrom R, et al. Developmental fate and cellular maturity encoded in human regulatory DNA landscapes. *Cell*. 2013; 154:888–903. [PubMed: 23953118]
- Suzuki T, Arumugam P, Sakagami T, Lachmann N, Chalk C, Sallèse A, Abe S, Trapnell C, Carey B, Moritz T, et al. Pulmonary macrophage transplantation therapy. *Nature*. 2014; 514:450–454. [PubMed: 25274301]
- Trapnell C, Pachter L, Salzberg SL. TopHat: discovering splice junctions with RNA-Seq. *Bioinformatics*. 2009; 25:1105–1111. [PubMed: 19289445]
- van Furth R, Cohn ZA, Hirsch JG, Humphrey JH, Spector WG, Langevoort HL. The mononuclear phagocyte system: a new classification of macrophages, monocytes, and their precursor cells. *Bull. World Health Organ.* 1972; 46:845–852. [PubMed: 4538544]
- Varol C, Vallon-Eberhard A, Elinav E, Aychek T, Shapira Y, Luche H, Fehling HJ, Hardt W-D, Shakhar G, Jung S. Intestinal lamina propria dendritic cell subsets have different origin and functions. *Immunity*. 2009; 31:502–512. [PubMed: 19733097]

- Virolainen M. Hematopoietic origin of macrophages as studied by chromosome markers in mice. *J. Exp. Med.* 1968; 127:943–952. [PubMed: 5655103]
- Winter DR, Amit I. The role of chromatin dynamics in immune cell development. *Immunol. Rev.* 2014; 261:9–22. [PubMed: 25123274]
- Yamanaka R, Barlow C, Lekstrom-Himes J, Castilla LH, Liu PP, Eckhaus M, Decker T, Wynshaw-Boris A, Xanthopoulos KG. Impaired granulopoiesis, myelodysplasia, and early lethality in CCAAT/enhancer binding protein epsilon-deficient mice. *Proc. Natl. Acad. Sci. USA.* 1997; 94:13187–13192. [PubMed: 9371821]
- Yang CY, Chen JB, Tsai TF, Tsai YC, Tsai CY, Liang PH, Hsu TL, Wu CY, Netea MG, Wong CH, Hsieh SL. CLEC4F is an inducible C-type lectin in F4/80-positive cells and is involved in alpha-galacto-sylceramide presentation in liver. *PLoS ONE.* 2013; 8:e65070. [PubMed: 23762286]
- Yona S, Kim K-W, Wolf Y, Mildner A, Varol D, Breker M, Strauss-Ayali D, Viukov S, Guillemins M, Misharin A, et al. Fate mapping reveals origins and dynamics of monocytes and tissue macrophages under homeostasis. *Immunity.* 2013; 38:79–91. [PubMed: 23273845]
- Zigmond E, Varol C, Farache J, Elmaliah E, Satpathy AT, Friedlander G, Mack M, Shpigel N, Boneca IG, Murphy KM, et al. Ly6C hi monocytes in the inflamed colon give rise to proinflammatory effector cells and migratory antigen-presenting cells. *Immunity.* 2012; 37:1076–1090. [PubMed: 23219392]
- Zigmond E, Bernshtein B, Friedlander G, Walker CR, Yona S, Kim KW, Brenner O, Krauthgamer R, Varol C, Müller W, Jung S. Macrophage-restricted interleukin-10 receptor deficiency, but not IL-10 deficiency, causes severe spontaneous colitis. *Immunity.* 2014; 40:720–733. [PubMed: 24792913]

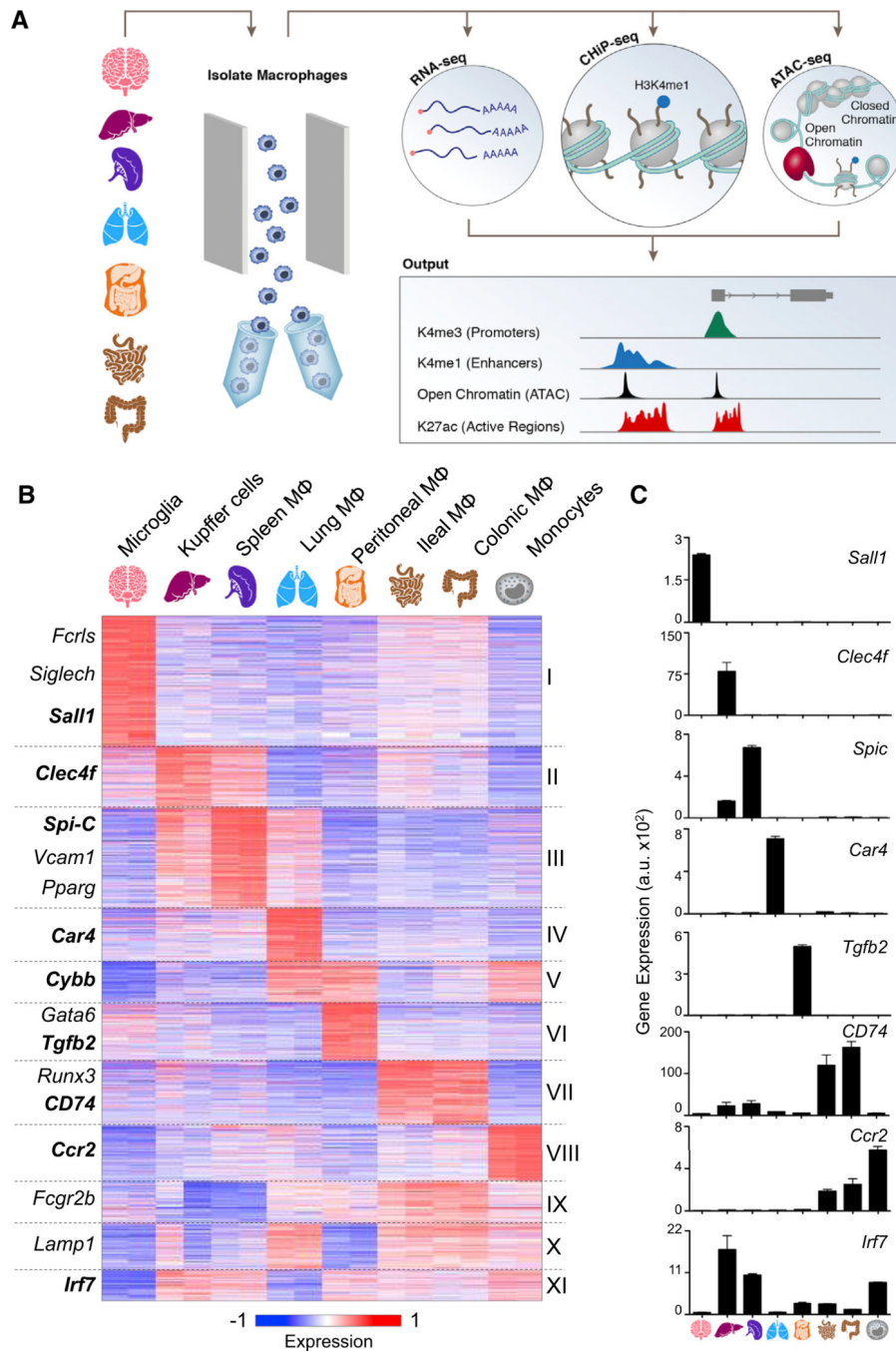


Figure 1. Tissue-Resident Macrophages Can Be Distinguished by Expression Patterns
 (A) Schematic for defining the global regulatory elements of tissue-resident macrophages, monocytes, and neutrophils isolated by the gating strategy (Data S1) and analyzed by sequencing data from high-throughput RNA-seq, ChIP-seq, and ATAC-seq. A representative genome browser output is shown.
 (B) K-means clustering ($K = 11$) of 3,348 differentially expressed genes in macrophages ($M\Phi$) and monocytes.
 (C) Bar charts showing gene expression levels (a.u. $\times 10^2$) for several genes across different cell types.

(C) Bar graphs of individual gene expression in arbitrary units (a.u.). Error bars indicate SEM.

See also Figure S1, Table S1, and Experimental Procedures.

Author Manuscript

Author Manuscript

Author Manuscript

Author Manuscript

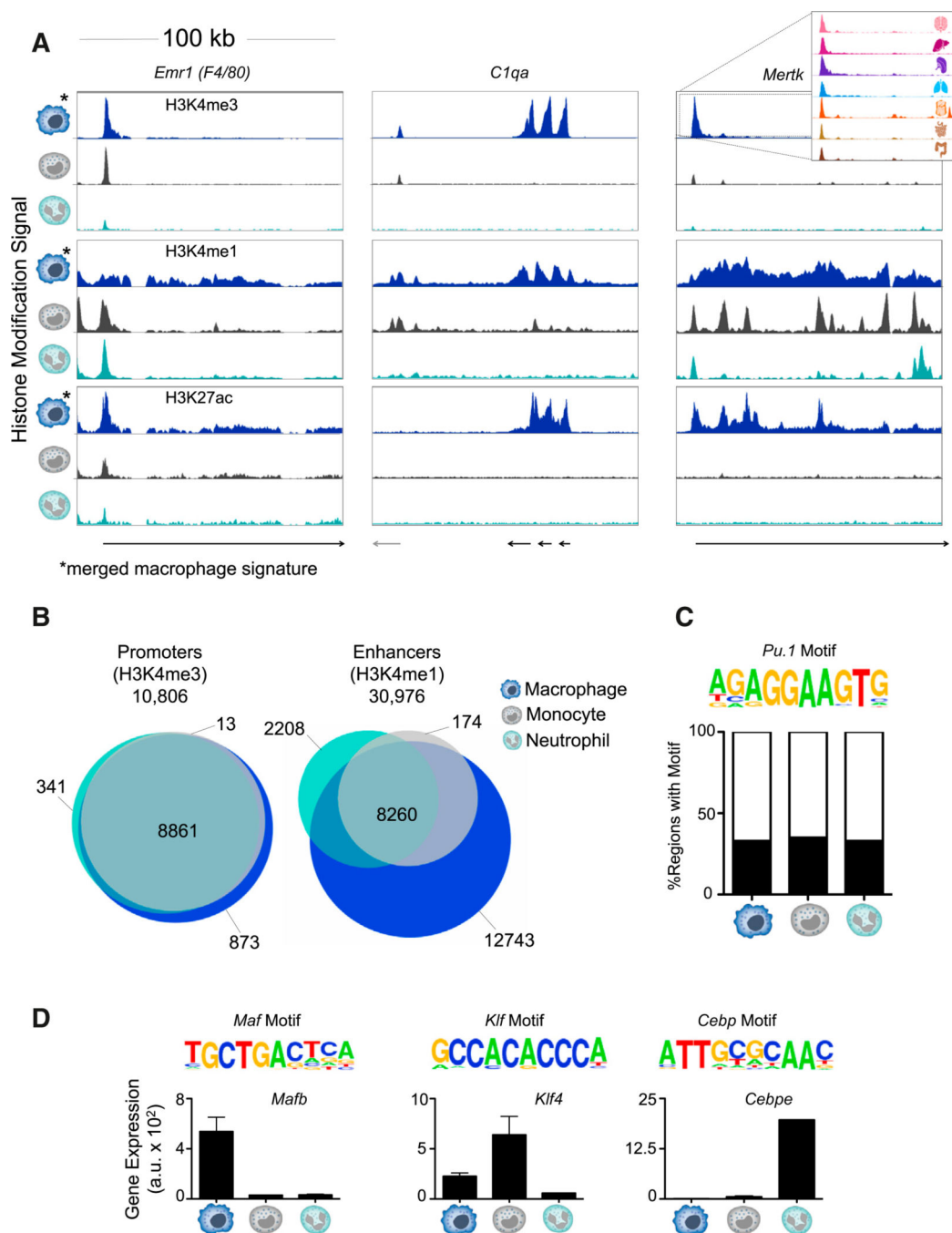


Figure 2. Comparing the Chromatin Landscape of Myeloid Cells Reveals Macrophage-Specific Enhancers

(A) Normalized profiles of H3K4me3, H3K4me1, and H3K27ac signal in 100 kilobase pair (kb) regions for monocytes, neutrophils, and “merged” macrophage signature of seven tissue-resident populations.

(B) Venn diagrams of the overlap of promoters (10,806; left) and enhancers (30,976; right) among macrophages, monocytes, and neutrophils.

(C) Representative motif of PU.1 enriched in H3K4me1-marked regions shared by all myeloid cell types ($p = 10^{-6}$) and percentage of regions with the motif in each cell type.

(D) Representative motifs of the indicated TF families found enriched in cell-type-specific H3K4me1-marked regions ($p < 10^{-5}$). Gene expression (a.u.) of the implicated family member. Error bars indicate SEM.
See also Figure S2 and Table S2.

Author Manuscript

Author Manuscript

Author Manuscript

Author Manuscript

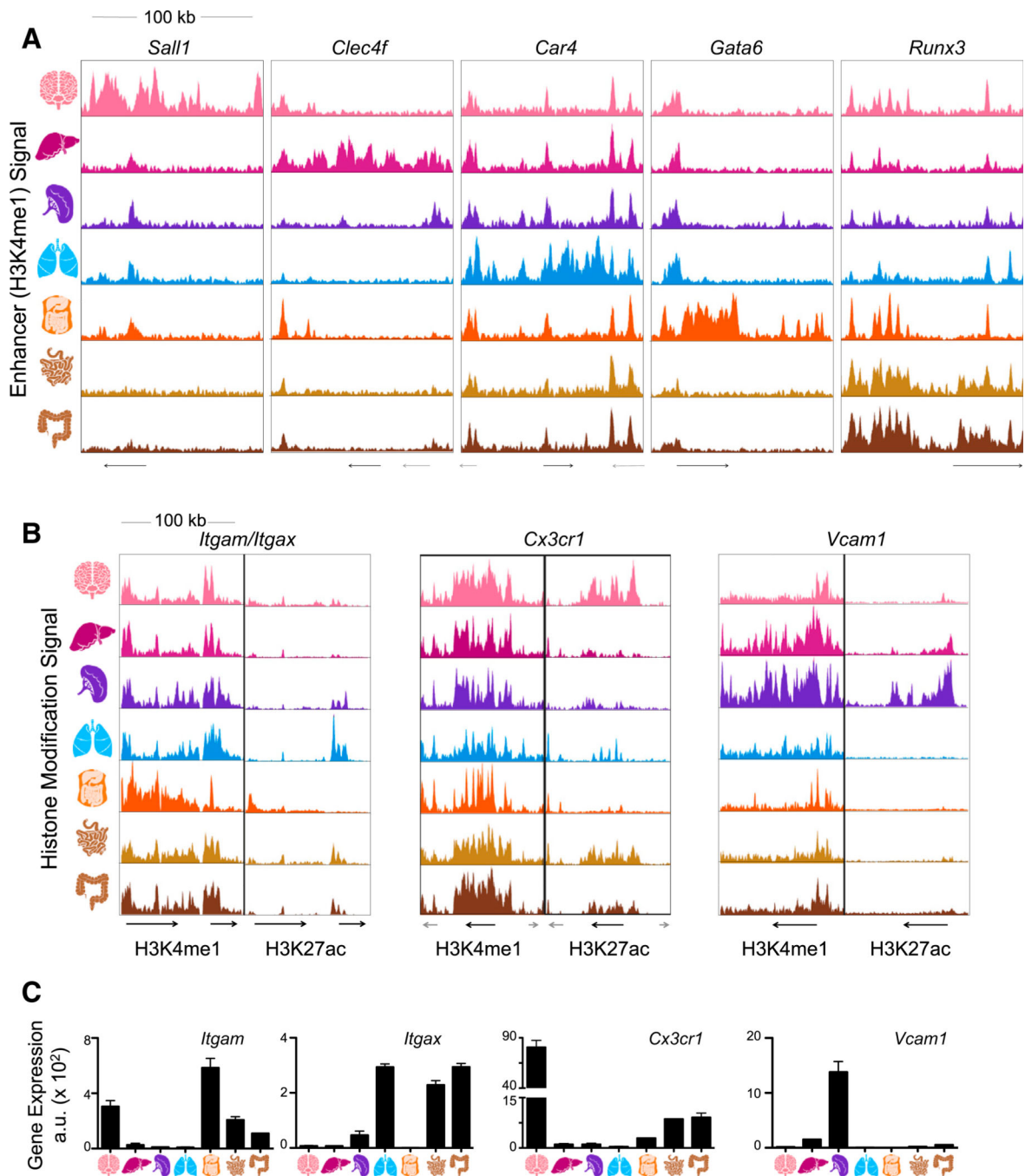


Figure 3. Tissue-Resident Macrophage Populations Have Unique Poised and Active Enhancers

(A) Normalized profiles of H3K4me1 signal for seven tissue-resident macrophage populations in 100 kb regions containing tissue-specific enhancers around the indicated genes.

(B) Normalized profiles of H3K27ac (right) signal in H3K4me1-marked (left) 100 kb regions containing the indicated genes.

(C) Bar graphs of expression (a.u.) for genes in loci of (B). Error bars indicate SEM.

See also Figure S4.

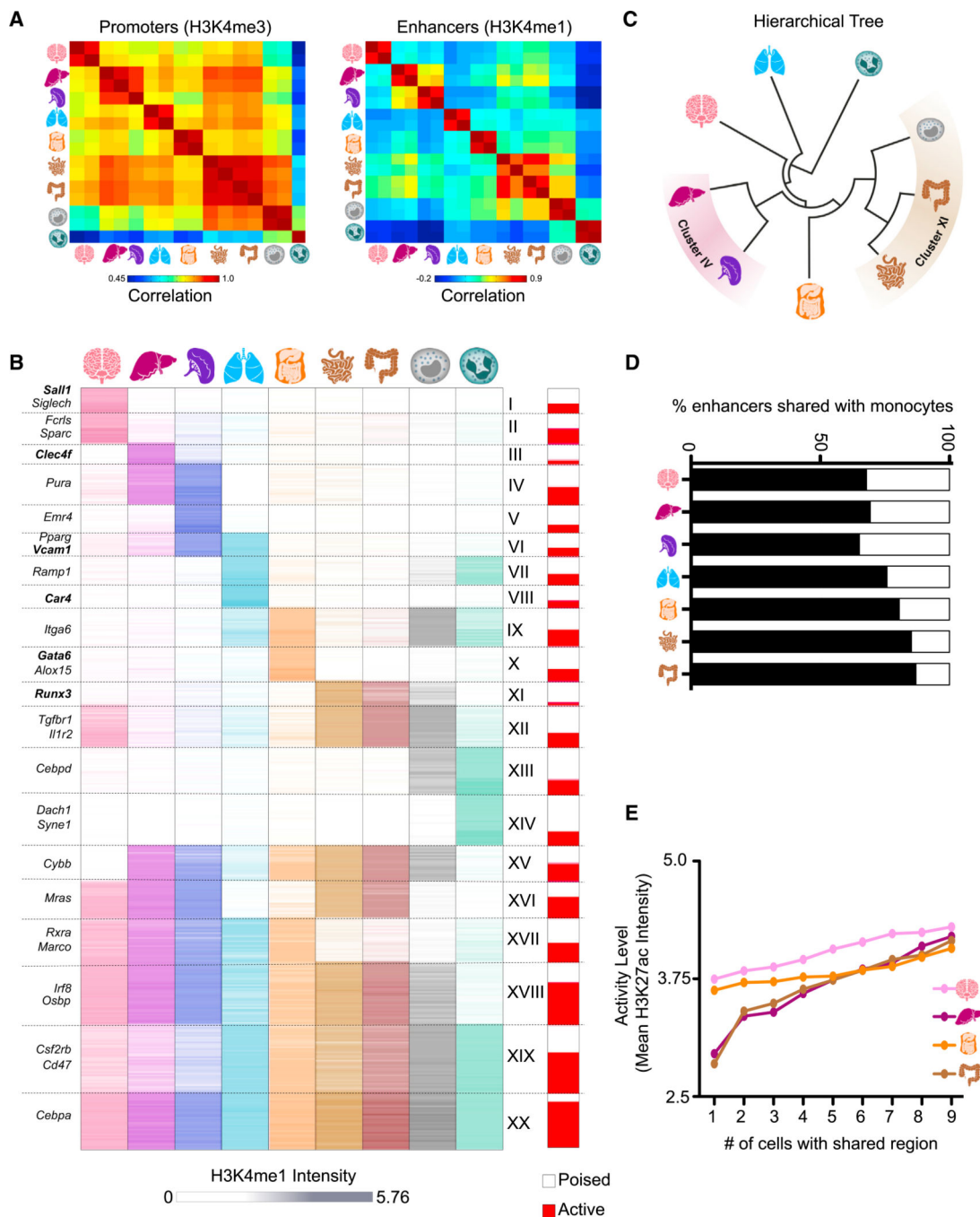


Figure 4. Tissue-Resident Macrophages Have Distinct Sets of Enhancers Determined by Ontogeny and Microenvironment
 (A) Pairwise correlations between replicates with respect to H3K4me3 read density in promoters (left) and H3K4me1 read density in enhancers (right).
 (B) K-means clustering (K = 20) of the H3K4me1 intensity in 30,976 high-confidence enhancer regions. The proportion of enhancers active (H3K27ac high) in at least one sample in each cluster is shown in red (right bar).
 (C) Hierarchical tree resulting from clustering on H3K4me1 intensity in enhancer regions.

(D) Percentage of H3K4me1-marked regions in monocytes shared with each tissue-resident macrophage.

(E) Line plots showing that enhancer activity level (mean H3K27ac intensity) increases with the number of samples that share the H3K4me1-marked regions.

See also Figures S3 and S4 and Table S3.

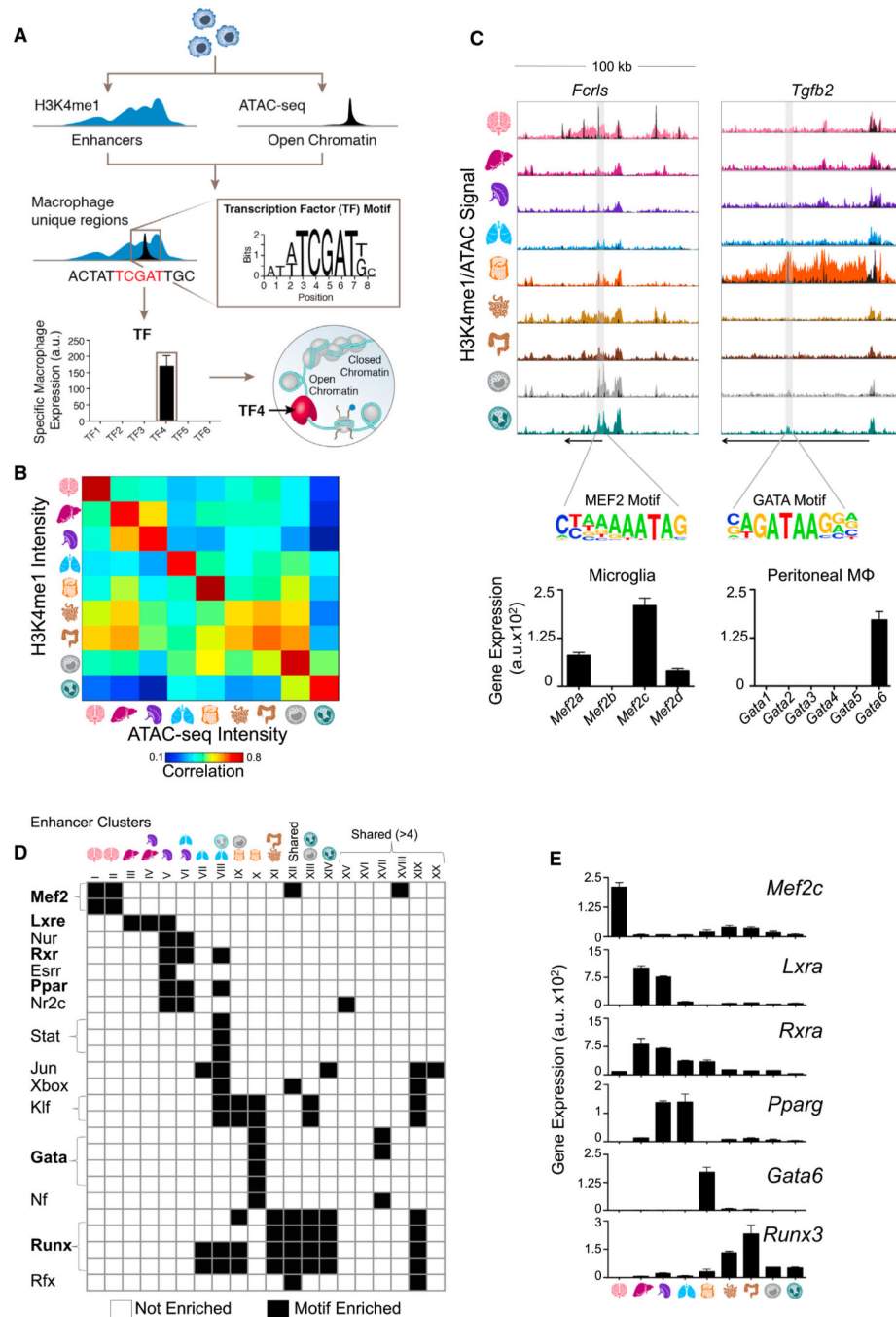


Figure 5. Identification of Candidate Regulators in Tissue-Resident Macrophage Enhancers Using ATAC-Seq

(A) Schematic of pipeline to identify candidate regulators of enhancers. For each cluster, enhancers are matched to ATAC-seq peaks, genomic sequence is lifted for input into the motif finder, and the enriched motif is matched to the TF family member with corresponding expression.

(B) Pairwise correlations between H3K4me1 and ATAC-seq intensity in enhancer regions.

(C) Normalized profiles of H3K4me1 signal in 100 kb regions with ATAC-seq peaks overlaid in black, containing tissue-specific enhancers around the indicated genes. Shaded

regions indicate location of the relevant motif. Bar graphs of gene expression (a.u.) for TF family members of Mef2 in microglia and Gata in peritoneal macrophages. Error bars indicate SEM.

(D) Heatmap of significantly enriched motifs ($p < 10^{-5}$) in H3K4me1-marked regions from each cluster in Figure 4B (see Table S4).

(E) Bar graphs show gene expression (a.u.) for candidate TFs that match motifs in (D). Error bars indicate SEM.

See also Figure S5 and Table S4.

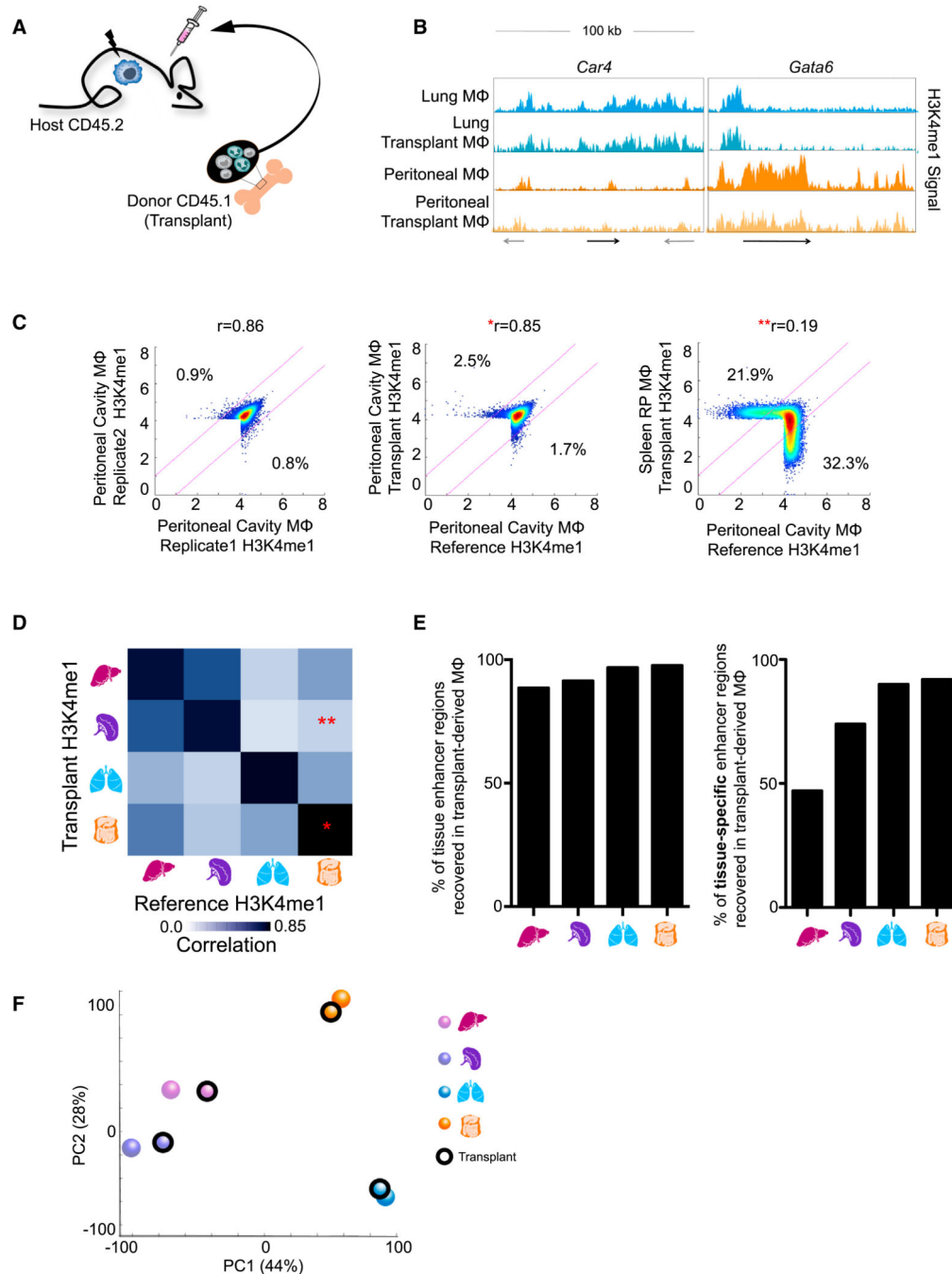


Figure 6. Microenvironment Signals Shape the Enhancer Landscape of Adult Bone-Marrow-Derived Macrophages

(A) Schematic of bone marrow transplant experiment.

(B) Normalized profiles of H3K4me1 signal of reference macrophages and transplant-derived macrophages both showing tissue-specific enhancers around *Car4* and *Gata6* in 100 kb regions.

(C) Density scatterplots of H3K4me1 intensity in H3K4me1-marked regions for reference peritoneal macrophages (x axis) between replicates (left), compared to peritoneal transplant-

derived macrophages (middle), or spleen transplant-derived macrophages (right). Regions of 2-fold differential (pink lines) and Pearson's correlation between samples are indicated.

(D) Pairwise correlations between transplant and reference macrophages with respect to H3K4me1 intensity in original and novel enhancers. The single asterisk (*) and double asterisk (**) correspond to the data shown in the respective plots from (C).

(E) Percent of total (left) or tissue-specific (right) reference macrophage H3K4me1-marked regions recovered by transplant-derived macrophages.

(F) PCA of H3K4me1 intensity showing transplanted macrophages group with their respective reference macrophages.

See also Figure S6.

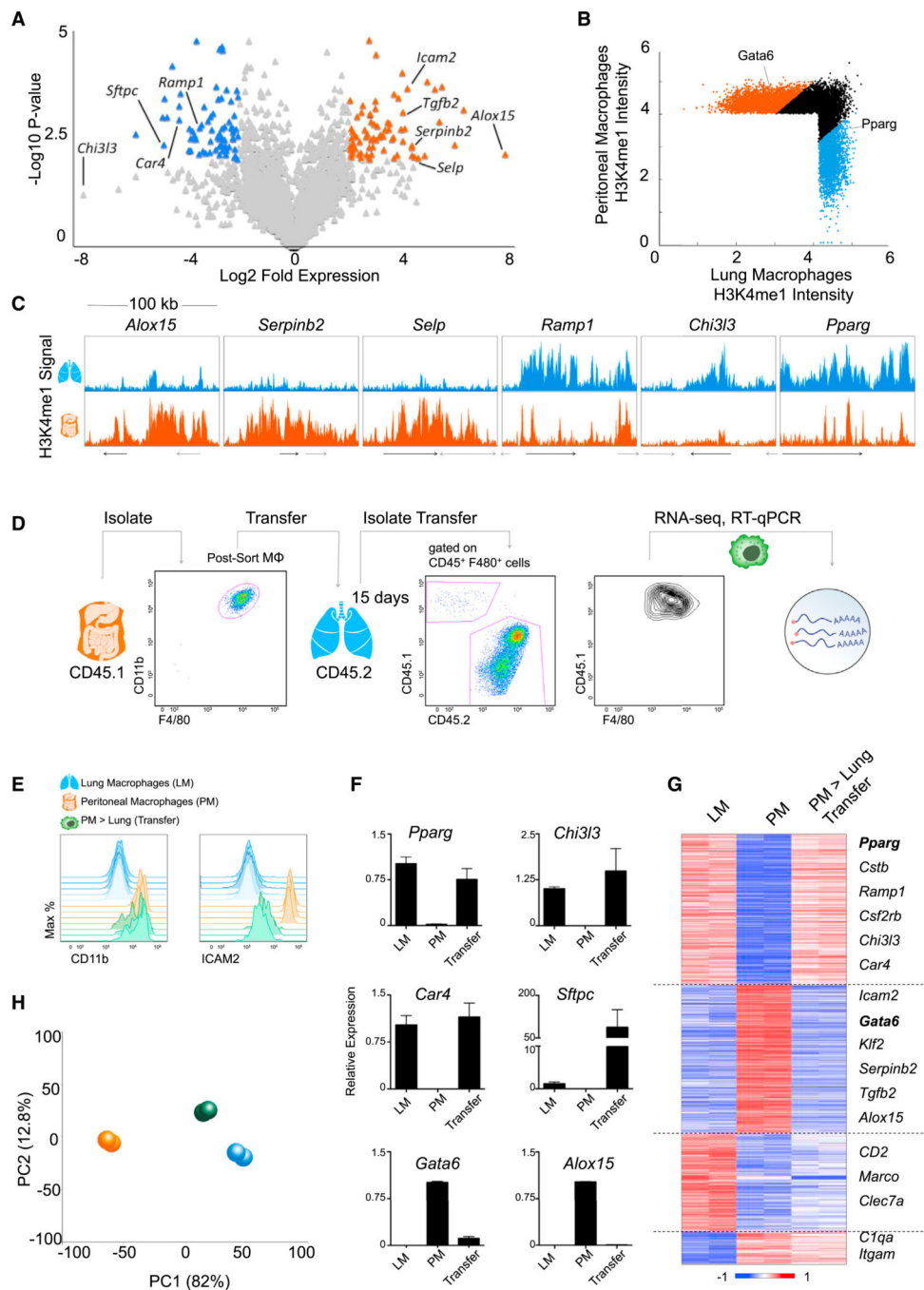


Figure 7. Differentiated Tissue-Resident Macrophages Are Reprogrammed by a New Microenvironment

(A) Volcano plot of relative expression in peritoneal (PM; right) and lung (LM; left) macrophages with differential (> 4-fold), statistically significant ($p < 0.01$) genes indicated in orange and blue, respectively.

(B) Scatterplot comparing intensity in H3K4me1-marked regions with differential PM (orange) and LM (blue) enhancers indicated.

(C) Normalized profiles of H3K4me1 signal of PM and LM in 100 kb regions.

(D) Schematic of transplant experiment: representative FACS plot of purified CD45.1⁺ PM prior to transfer and retrieved from host CD45.2⁺ lung.

(E–H) Resident LM, PM, and transferred macrophages recovered from the host lung tissue (PM > lung transfer) were analyzed by flow cytometry (E) and qRT-PCR (F). Error bars indicate SEM. RNA-seq from transferred macrophages was compared to reference macrophages for 1,014 differential genes sorted in a heatmap (G) and analyzed by PCA (H). See also Figure S7 and Table S5.